Korean J. Chem. Eng., **26**(3), 760-764 (2009)

Size-selective Pd nanoparticles stabilized by dialkylmorpholinium ionic liquids

Jong-Ho Cha*, Ki-Sub Kim, and Huen Lee*,†**

*Department of Chemical and Biomolecular Engineering, Korea Advanced Institute of Science and Technology, 335 Gwahangno, Yuseong-gu, Daejeon 305-701, Korea
**Department of Chemical and Biological Engineering, Chungju National University, 72 Daehangno, ChungCheongbuk-do, Chungju 380-702, Korea
(*Received 10 June 2008 • accepted 17 December 2008*)

Abstract−We have successfully synthesized palladium (Pd) nanoparticles (NPs) protected by dialkylmorpholinium ionic liquids (ILs) via chemical reduction. ATR-FTIR, UV, and NMR spectroscopies and transmission electron microscopy (TEM) were employed for characterization of the Pd NPs. The ILs effectively stabilized the Pd NPs, and the particle sizes were precisely controlled by the alkyl chain length of the cation in the ILs. The produced particles had a highly crystalline structure with a face-centered cubic (fcc) lattice. Broadening of the (111) plane in the X-ray diffraction (XRD) patterns was observed and the particle sizes calculated by Scherrer's equation were in good agreement with the TEM results. Additionally, UV, IR, and NMR spectra indicated that nano-sized particles were produced and ILs were bound to the surface of the NPs, thereby protecting the particles from aggregation.

Key words: Ionic Liquid, Morpholinium Salt, Palladium Nanoparticles, Size Control

INTRODUCTION

Recently, ionic liquids (ILs) have received growing attention as alternatives to traditional organic solvents in green industrial applications owing to their favorable properties [1-6]. Generally, ILs are in liquid form below 100 °C and consist of nitrogen-containing cations and inorganic anions. They are normally stable to air and water, and have low melting points, sometimes as low as −96 °C [7]. Furthermore, their physical properties strongly depend on either the alkyl chain length of the cation or specifically designed cation and anion. On the basis of these features of ILs, the reports on their applications to the synthesis of metal or inorganic nanostructures have gradually increased [8-14]. In particular, metal and semiconductor nanoparticles (NPs) have been widely employed to create advanced materials for use in electronics, sensors, and photonics, because of their unique optical and electrical properties. NPs have also served as precursors to form nanowires (NWs), nanorods (NRs), and nanosheets (NSs) [15,16]. The size of NPs strongly influences the properties of metals on a nano-scale. Thus, the infinitesimal and precise control of particle size, and a definite understanding of their chemical phenomena remains the urgent research task.

To date, most research on ILs has focused on 1,3-dialkylimidazolium salts, although an enormous number of new ILs have been synthesized. Thus, information on these salts for industrial applications is readily accessible. However, the products remain expensive, thus hindering wide ILs' applications despite their desirable features. In a previous work, we developed a new route to synthesize metal NPs using thiol-functionalized ionic liquids (TFILs) [17,18]. Although the approach based on TFILs has many advantages, it is still problematic in that the complex synthesis route of TFILs causes a decrease in the reproducibility of the IL products, which also results in low reproducibility of NPs. In a recent study, we also successfully synthesized Pd NPs with well-defined sizes by electrochemical reduction using a dialkylmorpholinium IL [19]. In this context, we synthesized the Pd NPs stabilized by N-butyl-N-methylmorpholinium tetrafluoroborate $[Mor_{1,4}][BF_4]$ and N-ethyl-N-methylmorpholinium tetrafluoroborate $[Mor_{1,2}][BF_4]$ via chemical reduction. The morpholinium ILs offer several advantages in the preparation of nano-materials: (1) The synthesis and purification procedures for the morpholinium ILs are much simpler than those for the TFILs and imidazolium salts; (2) The cost of raw material is less than that of imidazolium and ammonium salts; and (3) They possess good electrochemical and thermal properties. In the following, we describe the preparation and characteristics of $[Mor_{1,4}][BF_4]$- and $[Mor_{1,2}][BF_4]$-protected Pd NPs, and show that the particle size can be precisely controlled by the alkyl chain length of the cation.

†To whom correspondence should be addressed.
E-mail: h_lee@kaist.ac.kr

EXPERIMENTAL SECTION

1. Materials

The chemicals (source, grade) used in the syntheses of the ILs and Pd NPs are as follows: 4-methylmorpholine (Aldrich, 99%), bromoethane (Aldrich, 99%), 1-bromobutane (Aldrich, 99%), sodium tetrafluoroborate (Aldrich, 98%), sodium tetrachloropalladate (Aldrich, 98%), and sodium borohydride (Aldrich, 99%). Solvents include deionized water from a Millipore purification unit, acetone (Merck, 99.9%), acetonitrile (Merck, 99.9%), and ethanol (Merck, 99.9%). All chemicals were used without further treatment.

2. Preparation of Morpholinium ILs

Scheme 1 shows the synthetic procedures of $[Mor_{1,4}][BF_4]$ and $[Mor_{1,2}][BF_4]$ used in this study. The synthetic procedure was divided into two steps. The desired cation was formed and then the bromide anion was converted into the corresponding BF_4^- by a metathesis reaction.

2-1. Preparation of $[Mor_{1,2}][BF_4]$

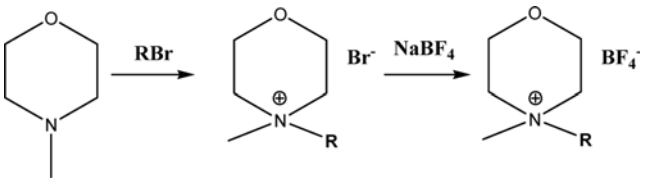

Scheme 1. Synthetic procedure of dialkylmorpholinium tetrafluoroborate.

4-Methylmorpholine (32.69 g, 0.30 mol) was mixed with an excess bromoethane in 200 mL of acetonitrile. The mixture was refluxed for 5 hours at 70 °C under N_2 atmosphere. After reaction, the acetonitrile was decanted from the solids and the mixture was recrystallized from acetone at room temperature to yield [$Mor_{1,2}$][Br], which was dried in vacuum. Then, [$Mor_{1,2}$][Br] (21.96 g, 0.20 mol) was reacted with sodium tetrafluoroborate (41.98 g, 0.20 mol) in acetone (25 °C, 24 hrs) to give [$Mor_{1,2}$][BF_4]. Sodium bromide was removed by filter paper. After rotor-evaporation, the product was dried under vacuum at 50 °C (35.55 g, 82.2%). The ^{1}H NMR and FAB mass spectra were recorded on a Bruker DMX 600 MHz NMR spectrometer and FAB mass JMS-HX110A, respectively. The possible presence of residual Br^- was examined by ionic chromatography. (System: Bio-LC DX-300 (Dionex, Sunny-vale, CA, USA); detector: suppressed conductivity (PED2); column: ICSep AN300 with ICSep ANSC guard). ^{1}H-NMR (500 MHz; Acetone; TMS) 4.14-4.04 (s, 4H), 3.79-3.75 (q, 4H), 3.67-3.61 (s, 3H), 3.39-3.36 (s, 2H), 1.50-1.46 (t, 3H). FAB MS: m/z=130 [$Mor_{1,2}$]$^+$. Br-content: 5.6 ppm.

2-2. Preparation of [$Mor_{1,4}$][BF_4]

The [$Mor_{1,4}$][BF_4] was prepared by repeating the above procedure with 1-bromobutane (yield 81.7%). ^{1}H-NMR (Acetone, δ/ppm, relative to TMS) 4.12-4.03 (m, 4H), 3.67-3.60 (m, 6H), 3.36 (s, 3H), 1.92-1.85 (m, 2H), 1.48-1.40 (m, 2H), 1.00-0.97 (t, 3H). FAB MS: m/z=158 [$Mor_{1,4}$]$^+$. Br-content: 145 ppm.

3. Preparation of Pd NPs

The chemical preparation of [$Mor_{1,2}$][BF_4]-protected Pd NPs was straightforward. An aqueous solution of [$Mor_{1,2}$][BF_4] (0.05 mmol) was added dropwise to an aqueous solution of Na_2PdCl_4 (0.01 mmol) with vigorous stirring at 70 °C. After stirring for approximately 10 minutes, an excess amount of sodium borohydride (0.05 mmol) was added dropwise to the previous solution. The reaction was carried out during 24 hours. The IL-protected Pd NPs were washed with ethanol and isolated by centrifugation. The same procedure was repeated with [$Mor_{1,4}$][BF_4] to produce [$Mor_{1,4}$][BF_4]-protected Pd NPs.

4. Characterization of Pd NPs

TEM images were obtained with a Phillips TECHNAI F-20 at beam energy of 200 kV. Samples were prepared by placing a corresponding nanocluster solution onto a copper-coated TEM grid and allowing the solvent to evaporate in ambient condition. The crystalline structure of Pd NPs was investigated by XRD on a Rigaku D/max-IIIC with Cu-Kα radiation (λ=1.5406 Å) at a generator voltage of 40 kV and a generator current of 40 mA. The UV-vis absorption spectra of colloidal dispersions before reduction and after reduction were recorded on a Varian CARY 100 conc. ^{1}H NMR and ATR-FTIR spectra of Pd NPs were recorded on a Bruker DMX 300 MHz spectrometer in acetone-d_6 solution and on a SensIR TravelIR portable, respectively.

RESULTS AND DISCUSSION

The precursor Na_2PdCl_4 and IL were first dissolved in water phase and Pd ions were then reduced by $NaBH_4$ at 70 °C. At this time, the solution turned from pale brown to black. The reaction was monitored by UV-visible absorption spectra (Fig. 1). The mixed solution of [$Mor_{1,4}$][BF_4] and Na_2PdCl_4 before reflux shows peaks at 212 and 238 nm due to ligand-to-metal charge transfer transition of Pd^{2+} complexes. On the other hand, Na_2PdCl_4 solution without the IL exhibits absorption peaks at 207 and 235 nm. The red shifts strongly suggest that Cl^- and/or H_2O of Pd complexes in Na_2PdCl_4 solution are replaced by the IL, and new Pd^{2+} complexes consisting of Pd^{2+} ions and the IL are formed. After the chemical reaction, however,

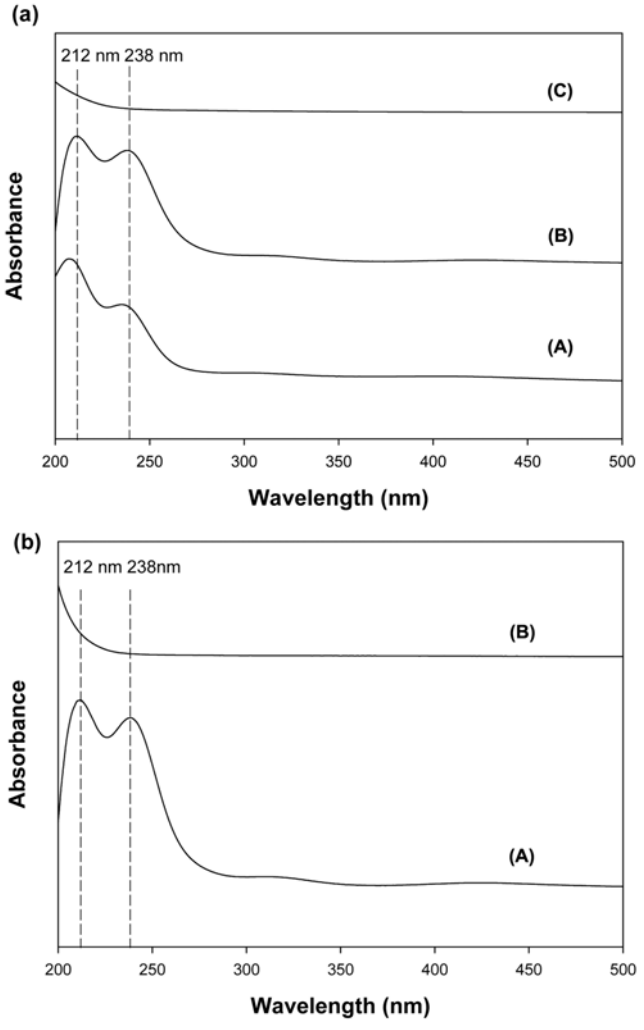

Fig. 1. (a) UV-vis spectra of the Na_2PdCl_4 aqueous solution (A), and mixed solution of [$Mor_{1,4}$][BF_4] and Na_2PdCl_4 before reflux (B) and the solution of [$Mor_{1,4}$][BF_4] with Na_2PdCl_4 after 24 h for the chemical reaction (C), and (b) UV-vis spectra of the mixed solution of [$Mor_{1,2}$][BF_4] and Na_2PdCl_4 before reflux (A), and the solution of [$Mor_{1,2}$][BF_4] with Na_2PdCl_4 after 24 h for the chemical reaction (B).

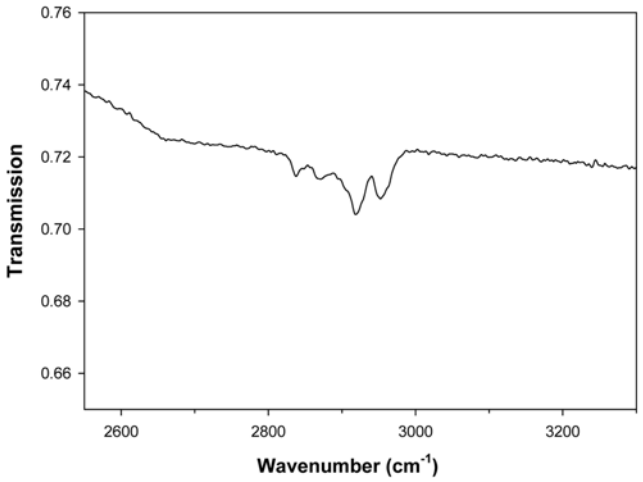

Fig. 2. ATR-FTIR spectrum of purified $[Mor_{1,2}][BF_4]$-Pd NPs.

broad absorption is shown and well-defined surface plasmon bands do not appear, which is typical of nanometer-sized Pd particles [20]. In the ^{1}H NMR spectrum, the proton signals for purified Pd NPs ($[Mor_{1,2}][BF_4]$-Pd) appear at positions that are almost identical to those of $[Mor_{1,2}][BF_4]$, itself [21]. Additionally, C-H aliphatic vibration near 2,900 cm^{-1} in the FT-IR spectrum is observed for IL-protected Pd NPs (Fig. 2). These results demonstrate that the IL coexists with Pd and is possibly absorbed on the metal surface.

The average sizes and size distributions of the Pd NPs were determined by TEM. Fig. 3 shows that the average sizes are 3.8 and 4.2 nm and the standard deviation are 0.6 and 0.9 nm for $[Mor_{1,4}][BF_4]$-, and $[Mor_{1,2}][BF_4]$-protected Pd NPs, respectively. It can be seen that the average size of the Pd NPs increases with a decrease in the carbon-chain length of the cation in the IL. Thus, the particle size becomes smaller in the order of $[Mor_{1,4}][BF_4]$ and $[Mor_{1,2}][BF_4]$. This indicates that the length of the alkyl chain in the stabilizers strongly affects the average size. In fact, variation of the length adjusts the polarity of the stabilizer, which influences the hydrophobic interaction between the stabilizer and Pd atom. Stronger hydrophobic interaction induced by the low polarity of the stabilizer with a longer carbon chain results in more Pd atoms remaining on the particle surface and suppression of the growth of Pd NPs. Thus, the diameter of the resulting Pd NPs becomes smaller under the protection of the IL containing long alkyl chain. In addition to TEM photograph analyses, the crystallinity and crystal structure of the Pd NPs were investigated by XRD analysis. As shown in Fig. 4, the resulting NPs with $[Mor_{1,4}][BF_4]$, and $[Mor_{1,2}][BF_4]$ show peaks at around 40°, 46°, 68°, and 82°. These peaks correspond to (111), (200), (220), and (311) crystalline planes of the face-centered cubic (fcc) lattice, respectively. The XRD pattern also shows that the in-

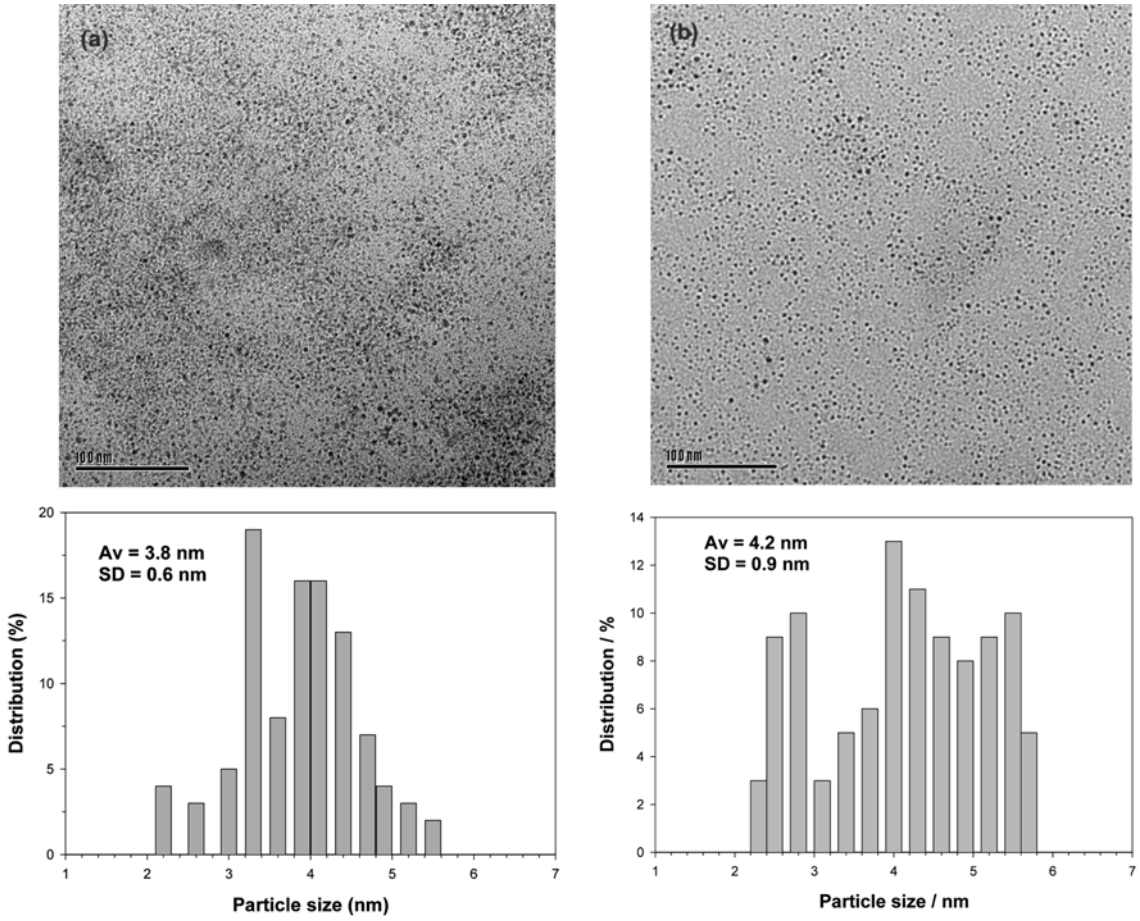

Fig. 3. TEM photographs and size distribution diagrams of resulting NPs: (a) $[Mor_{1,4}][BF_4]$-protected Pd NPs, and (b) $[Mor_{1,2}][BF_4]$-protected Pd NPs (scale bars of 100 nm).

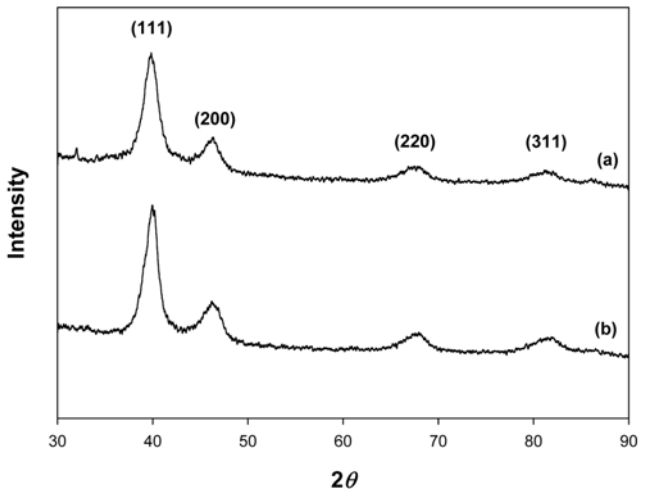

Fig. 4. The XRD patterns of Pd NPs: (a) $[Mor_{1,4}][BF_4]$-Pd NPs, and (b) $[Mor_{1,2}][BF_4]$-Pd NPs.

tensity of the peaks decreases as the alkyl chain length of the cation is increased in the ILs protecting the Pd NPs. At the same time, the X-ray reflection planes in the $[Mor_{1,4}][BF_4]$-protected NPs are slightly broadened relative to the $[Mor_{1,2}][BF_4]$-protected NPs. This broadening provides useful information on the particle sizes. In particular, from the (111) plane we were able to calculate the average sizes of the Pd NPs using Scherrer's equation, obtaining values of 4.0 and 4.2 nm for $[Mor_{1,4}][BF_4]$- and $[Mor_{1,2}][BF_4]$-protected NPs, respectively. These results are in good agreement with measurements taken from TEM photographs. Accordingly, it becomes clear that with a decrease in the particle size, the crystallinity of the Pd NPs is decreased, as previously reported by Teranishi et al. for PVP-protected Pd NPs [22].

The dialkylmorpholinium ILs are also applicable to the preparation of various metal NPs. Fig. 5 shows TEM photographs of $[Mor_{1,4}][BF_4]$-protected Ag and Pt NPs prepared under the identical experimental conditions above experiments. Their particle sizes and standard deviations are found to be 4.6 and 1.1 nm, and 4.8 and 1.5 nm, for Ag and Pt NPs, respectively. However, the Ag and Pt NPs show wider size distributions compared to Pd NPs, indicating that the Pd NPs are more efficiently protected. In addition, the morpholinium salt with bromide anion as well as with BF_4^- successfully stabilizes the Pd NPs. A TEM photograph and a standard deviation diagram of $[Mor_{1,12}][Br]$-protected Pd NPs are presented in Fig. 5(c).

CONCLUSION

We have described the protection of metal NPs by dialkylmorpholinium ILs. The ILs act as an effective stabilizer of Pd NPs in water phase. The produced NPs show average sizes of 3.8 and 4.2 nm for $[Mor_{1,4}][BF_4]$-, and $[Mor_{1,2}][BF_4]$-protected Pd NPs, respectively, and the sizes were precisely controlled by the alkyl chain length of the cation. In addition, Ag and Pt NPs were also well produced by the protection of ILs without any agglomerations. However, their particles showed a wider size distribution relative to that of Pd NPs. The present results suggest that the ILs can lead to effective stabilization to various metal NPs. In research to date, numerous stabilizers have been employed to prepare various nanostructures. However, the simple procedure presented here to prepare morpholinium ILs allows for simpler synthesis of the task-specific

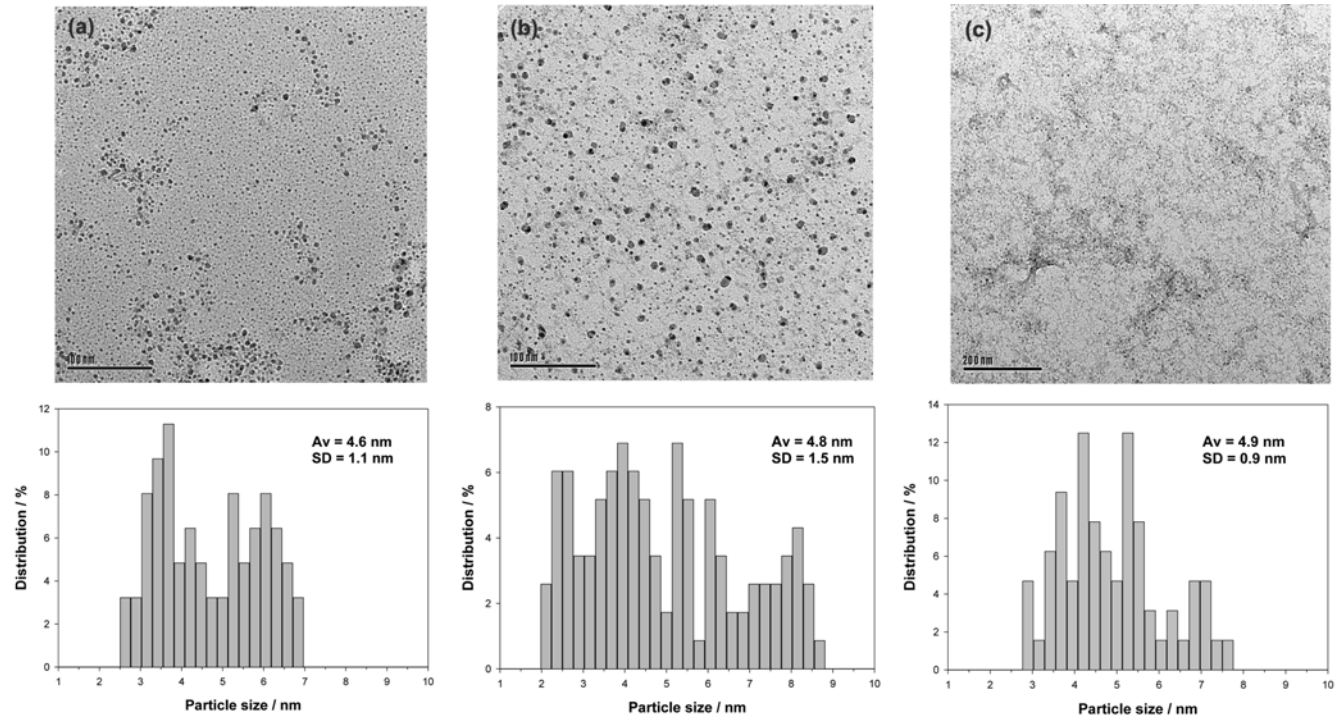

Fig. 5. TEM photographs and size distribution diagrams of resulting NPs: (a) $[Mor_{1,4}][BF_4]$-protected Ag NPs, (b) $[Mor_{1,4}][BF_4]$-protected Pt NPs, and (c) $[Mor_{1,12}][Br]$-protected Pd NPs (scale bars of 100 nm for (a) and (b), and 200 nm for (c)).

IL possessing various physicochemical properties by varying the cationic or anionic conformation. This will allow wider application of ILs in the preparation of various nanostructures.

ACKNOWLEDGMENT

This work was supported by the Korea Science & Engineering Foundation (KOSEF) grant (WCU program, 31-2008-000-10055-0) funded by the Ministry of Education and Science & Technology (MEST) and partially funded by the Brain Korea 21 Porject. Prof. Kim (Ki-Sub Kim) acknowledges support from the Korea Research Foundation Grant funded by the Korean Government (KRF-2008-331-D00110). We are grateful to KBSI (Korea Basic Science Institute) for assistance with NMR, FAB mass, and ion chromatography.

REFERENCES

1. K.-S. Kim, S. Choi, D. Demberelnyamba, H. Lee, J. Oh, B.-B. Lee and S.-J. Mun, *Chem. Commun*., 828 (2004).
2. K.-S. Kim, S.-Y. Park, S.-H. Yeon and H. Lee, *Electrochimica Acta.*, **50**, 5673 (2005).
3. S.-H. Yeon, K.-S. Kim, S. Choi, H. Lee, H. S. Kim and H. Kim, *Electrochimica Acta.*, **50**, 5399 (2005).
4. K.-S. Kim, B.-K. Shin, H. Lee and F. Ziegler, *Fluid Phase Equilibia*, **218**, 215 (2004)
5. T. Welton, *Chem. Rev.*, **99**, 2071 (1999).
6. K. N. Marsh, A. Deev, A. C-T. Wu, E. Tran and A. Klamt, *Korean J. Chem. Eng*., **19**, 357 (2002).
7. K. R. Seddon, A. Stark and M.-J. Torres, *Pure Appl. Chem.*, **72**, 2275 (2000).
8. J. Dupont, G. S. Fonseca, A. P. Umpierre, P. F. P. Fichtner and S. R. Teixeira, *J. Am. Chem. Soc*., **124**, 4228 (2002).
9. J. Huang, T. Jiang, B. Han, H. Gao, Y. Chang, G. Zhao and W. Wu, *Chem. Commun.*, 1654 (2003).
10. Y.-J. Zhu, W.-W. Wang, R.-J. Qi and X.-L. Hu, *Angew. Chem. Int. Ed.*, **43**, 1410 (2004).
11. K.-S. Kim, S. Choi, J.-H. Cha, S.-H. Yeon and H. Lee, *J. Mater. Chem*., **16**, 1315 (2006).
12. E. R. Parnham and R. E. Morris, *J. Am. Chem. Soc.*, **128**, 2204 (2006).
13. K. Ding, Z. Miao, Z. Liu, Z. Zhang, B. Han, G. An, S. Miao and Y. Xie, *J. Am. Chem. Soc.*, **129**, 6362 (2007).
14. S. Shimano, H. Zhou and I. Honma, *Chem. Mater.*, **19**, 5216 (2007).
15. Z. Tang, N. A. Kotov and M. Giersig, *Science*, **297**, 237 (2002).
16. Z. Tang, B. Ozturk, Y. Wang and N. A. Kotov, *J. Phys. Chem. B*, **108**, 6927 (2004).
17. K.-S. Kim, D. Demberelnyamba and H. Lee, *Langmuir*, **20**, 556 (2004).
18. K.-S. Kim, D. Demberelnyamba, S.-H. Yeon, S. Choi, J.-H Cha and H. Lee, *Korean J. Chem. Eng.*, **22**, 717 (2005).
19. J.-H. Cha, K.-S. Kim, S. Choi, S.-H. Yeon, H. Lee, C.-S. Lee and J.-J. Shim, *Korean J. Chem. Eng.*, **24**, 1089 (2007).
20. J. A. Creighton and D. S. Eadon, *J. Chem. Soc. Faraday Trans.*, **87**, 3881 (1991).
21. ^{1}H-NMR (500 MHz; Acetone; TMS) 4.15-4.09 (m, 4H), 3.89-3.82 (q, 4H), 3.73-3.70 (t, 3H), 3.45 (s, 2H), 1.50-1.46(m, 3H).
22. T. Teranishi and M. Miyake, *Chem. Mater.*, **10**, 594 (1998).